Inside the horizon with AdS/CFT

Per Kraus

Department of Physics and Astronomy, UCLA, Los Angeles, California 90095, USA

Hirosi Ooguri

California Institute of Technology 452-48, Pasadena, California 91125, USA

Stephen Shenker

Department of Physics, Stanford University, Stanford, California 94305, USA

Using the eternal BTZ black hole as a concrete example, we show how spacelike singularities and horizons can be described in terms of AdS/CFT amplitudes. Our approach is based on analytically continuing amplitudes defined in a Euclidean signature. This procedure yields finite Lorentzian amplitudes. The naive divergences associated with the Milne type singularity of BTZ black holes are regulated by an $i\epsilon$ prescription inherent in the analytic continuation and a cancellation between future and past singularities. The boundary description corresponds to a tensor product of two CFTs in an entangled state, as in previous work. We give two bulk descriptions corresponding to two different analytic continuations. In the first, only regions outside the horizon appear explicitly, and so amplitudes are manifestly finite. In the second, regions behind the horizon and on both sides of the singularity appear, thus yielding finite amplitudes for virtual particles propagating through the black hole singularity. This equivalence between descriptions only outside and both inside and outside the horizon is reminiscent of the ideas of black hole complementarity.

I. INTRODUCTION

It has been a long-standing goal of string or M theory to understand the singularities in spacetime geometry that afflict classical general relativity. Much progress has been made in understanding static time independent singularities. For example, orbifolds [1], conifolds [2], and enhancons [3] each represent a successful resolution of a classical singularity, the latter two requiring nonperturbative (in g_s) phenomena.

Much less is known about the fate of nonstatic, spacelike or null singularities. These are crucial in cosmology and include the Friedmann-Robertson-Walker (FRW) big bang and big crunch singularities. The singularity at the center of a black hole is of this type as well. The conventional wisdom has been that nonperturbative phenomena would come into play near these singularities. Recently real calculations have been done in perturbative string theory in mild big bang or big crunch type backgrounds [4–12]. In the examples of cosmological singularities constructed as time dependent orbifolds of Minkowski space, the work of Ref. [8] showed that tree level amplitudes diverge, due to infinite blueshifts at the singularities. References [13,14] discussed the physical meaning of these results and argued that in general nonperturbative phenomena should be expected around such points.

Enough progress has been made in string or M theory so that algorithmically complete nonperturbative definitions of the theory exist in certain backgrounds. These include matrix theory [15], the AdS conformal field theory (CFT) correspondence [16–18] and its relatives, and, to some extent, string field theory [19]. The hope exists that such definitions could cast some light on the spacelike singularity problem.

The AdS/CFT correspondence seems particularly well suited to this question because of the great success it has had in elucidating the physics of black holes. In particular the region outside the horizon of an AdS-Schwarzschild black hole is represented holographically by the boundary CFT at finite temperature [20].

The black hole singularity is behind the horizon and so at first glance the boundary CFT does not seem able to say anything about it. But on closer examination [21–23], the boundary degrees of freedom do seem to be able to probe the region of spacetime behind the horizon, implementing the redundancy of description implied by the ideas of black hole complementarity [24]. A particularly clear example of this, building on an old observation of Israel [25], involves the boundary description of an eternal AdS-Schwarzschild black hole. Such a geometry has two disconnected asymptotic boundaries, both approximately AdS. Not surprisingly, then, the holographic description of this geometry involves *two* decoupled CFTs, one on each boundary [26,27,22]. The only coupling between CFTs is via the entangled state $|\Psi\rangle$, referred to as the Hartle-Hawking state, in which all expectation values are taken. Correlation functions in one CFT reproduce the thermal results for correlators outside the horizon of the black hole; the black hole entropy in this formalism is the entanglement entropy of the state $|\Psi\rangle$.[1] But correlation functions involving the expectation values in $|\Psi\rangle$ of operators in both CFTs should, as Maldacena [22] has argued, contain some information about the geometry behind the horizon.

---

[1]This formalism has recently been applied to the question of the quantum consistency of de Sitter space by Goheer, Kleban, and Susskind [28].

The goal of this paper, building especially on the work of Ref. [22], is to understand more carefully what kind of behind the horizon information is contained in such correlators and, in particular, what information about the singularity can be obtained from them.

For simplicity we focus on the $2+1$ case [29], i.e., the Bañados-Teitelboim-Zanelli (BTZ) black hole [30], which is an orbifold of AdS. The spacelike singularity of the nonextremal, nonrotating BTZ black hole is given locally by a boost orbifold of two-dimensional Minkowski space times a spacelike line. The two-dimensional piece is referred to as the Milne universe, and describes contracting and expanding cones touching at a singularity. The null singularity studied in Ref. [8] is identical to the singularity of the zero mass limit of the BTZ black hole.

The natural way to define Lorentzian correlators of boundary operators in either the bulk or boundary description is via analytic continuation from the Euclidean theory. Because of the freedom to choose integration contours we show that it is possible to describe a given amplitude as being determined by information completely outside the horizon, or alternatively but equivalently as being determined by information both inside and outside the horizon. This is reminiscent of the concept of black hole complementarity [24].[2]

As we will argue later, these continued amplitudes are expected to be finite and the perturbation expansion for them well behaved. We then must ask what happens to the breakdown expected from the singularities. In the description involving data only outside the horizon there is nothing to explain. In the description that probes behind the horizon we find, at least in one case, that the singular behavior cancels between the future and past singularities.

Another question that arises concerns the intricate boundary structure of Lorentzian BTZs. We will argue that despite the apparent existence of an infinite number of boundary components the boundary CFTs only lie on the original two boundaries.

We now turn to a more detailed description of the content of the paper. Our main task is to show how to explicitly perform the analytic continuation of AdS/CFT amplitudes from Euclidean to Lorentzian signature. In principle, we could try to do this directly at the level of the string worldsheet path integral, but we will instead consider the simpler case of supergravity amplitudes, as these are sufficient for our purposes. The idea is to start from some Euclidean supergravity amplitude, defined in position space as an integration over the positions of interaction vertices, which are in turn connected by various bulk-boundary and bulk-bulk propagators. The amplitudes are labeled by points on the Euclidean boundary torus, corresponding to the locations of operators in the boundary CFT.

As we proceed to continue the boundary points to the Lorentzian section, we will have to deform the contour on which the interaction vertices are integrated. This is because

the propagators have singularities in the complex plane, and we must deform the contour to avoid encountering the singularities. We obtain a Lorentzian interpretation from the form of the final contour, as well as an $i\epsilon$ prescription for integrating around the various singularities. Since there is some freedom in how we deform the integration contour, there are a number of different possible Lorentzian interpretations of the same analytically continued amplitudes, of which we explore two.

The first corresponds to doing the natural contour deformation with respect to integration over time in the BTZ coordinates, which corresponds to a Killing vector of the BTZ geometry. This gives a Lorentzian amplitude in which we integrate vertices over two coordinate patches outside the horizon (the left and right wedges of the Penrose diagram), as well as over two imaginary time segments which can be thought of as imposing the Hartle-Hawking wave function. In this description, no explicit reference is made to the region behind the horizon or to the singularity, and the finiteness of the amplitudes is manifest. The analogous continuation of boundary CFT amplitudes naturally leads to a tensor product of two entangled CFTs associated to the boundaries of the two coordinate patches, as in previous work [22,26,27,31]. So the bulk and boundary description match up nicely, and in neither do the other components of the BTZ geometry make an appearance.

The first continuation just described is analogous to continuing flat space amplitudes with respect to Rindler time, whereas our second continuation is analogous to continuing with respect to Minkowski time. For the latter case we introduce Kruskal coordinates for BTZ, and perform the natural continuation with respect to Kruskal time. This leads to a Lorentzian description in which we integrate over a greater portion of the BTZ geometry than before, including the BTZ singularity and beyond. The $i\epsilon$ prescription provided by the analytic continuation tells us how to integrate the vertices over the BTZ singularities. Since we effectively go around the singularity in the complex plane, a naively divergent result is replaced by a finite but complex result. However, recalling that BTZ has both past and future singularities, we show that unphysical imaginary parts cancel between the two singularities, at least in some cases. The $i\epsilon$ prescription and the cancellation between past and future singularities are the mechanisms that seem to allow a well behaved boundary theory to describe the singular geometry behind the horizon.

The possibility of choosing two different contours to describe the same amplitude, one involving data only outside the horizon, the other involving data behind the horizon, is reminiscent of black hole complementarity ideas. It is striking that amplitudes apparently related solely to phenomena outside the horizon can also be used to reconstruct many properties of the geometry behind the horizon as well as some other phenomena that occur there. We note that these are phenomena that do not involve breakdown in the perturbative description.

The remainder of this paper is organized as follows. In Sec. II we review the BTZ geometry, its bulk-boundary propagator, and the reason why we might expect divergences from the BTZ singularity. In Sec. III we begin investigating

---

[2]Another indication of complementarity in this formalism has been discussed in Ref. [22].

the singularity with two point functions and their relation to spacelike geodesics in the bulk, although we later see that this approach has its limitations. Arguments for the finiteness of analytically continued amplitudes are given in Sec. IV. The prescription for the analytic continuation from the point of view of boundary CFT is reviewed in Sec. V. Before discussing the analytic continuation in the bulk BTZ geometry, sample computations in Minkowski spacetime are given in Sec. VI. Finally, in Sec. VII we study the BTZ amplitudes in two different ways by continuing with respect to BTZ time and Kruskal time, and then discuss the results. As this manuscript was being finished Ref. [32] appeared, which has significant overlap with this work.

II. REVIEW OF BTZ BLACK HOLE

A. Geometry

Let us recall the construction of the nonrotating BTZ black hole. More details, including the rotating case, can be found in Refs. [30,31]. Previous work on string theory on BTZ includes Refs. [22,31,33,34]. The starting point is AdS_3 described as a hyperboloid embedded in a flat spacetime with signature $(+, +, --)$:

$$x_0^2 + x_1^2 - x_2^2 - x_3^2 = 1. \qquad (2.1)$$

We are setting the AdS_3 length scale to unity. As usual, we will actually work with the simply connected covering space of Eq. (2.1). The BTZ solution is obtained by identifying points by a boost

$$x_1 \pm x_2 \cong e^{\pm 2\pi r_+}(x_1 \pm x_2). \qquad (2.2)$$

This will result in a nonrotating black hole of mass $M = r_+^2/8G_N$. The line of fixed points at $x_1 = x_2 = 0$ is the black hole singularity. The local geometry near the singularity is described by the Milne universe times a line. Indeed, solving Eq. (2.1) for x_3 near the line of fixed points yields

$$ds^2 \sim -dx_1^2 + dx_2^2 + \frac{dx_0^2}{1 - x_0^2}. \qquad (2.3)$$

The boost identification in the (x_1, x_2) plane defines the Milne universe.

To write coordinates that display the symmetries of the spacetime, we break up AdS_3 into the following three types of regions:

$$\text{region 1:} \quad x_1^2 - x_2^2 \geqslant 0, \quad x_0^2 - x_3^2 \leqslant 0,$$

$$\text{region 2:} \quad x_1^2 - x_2^2 \geqslant 0, \quad x_0^2 - x_3^2 \geqslant 0, \qquad (2.4)$$

$$\text{region 3:} \quad x_1^2 - x_2^2 \leqslant 0, \quad x_0^2 - x_3^2 \geqslant 0.$$

We then cover each region by four separate coordinate patches, corresponding to the values of $\eta_{1,2} = \pm 1$.

Region 1:

$$x_1 \pm x_2 = \eta_1 \frac{r}{r_+} e^{\pm r_+ \phi}, \qquad (25)$$

$$x_3 \pm x_0 = \eta_2 \frac{\sqrt{r^2 - r_+^2}}{r_+} e^{\pm r_+ t}.$$

Region 2:

$$x_1 \pm x_2 = \eta_1 \frac{r}{r_+} e^{\pm r_+ \phi},$$

$$\qquad\qquad\qquad\qquad (2.6)$$

$$x_3 \pm x_0 = \eta_2 \frac{\sqrt{r_+^2 - r^2}}{r_+} e^{\pm r_+ t}.$$

Region 3:

$$x_1 \pm x_2 = \eta_1 \frac{\sqrt{r^2 - r_+^2}}{r_+} e^{\pm r_+ t},$$

$$\qquad\qquad\qquad\qquad (2.7)$$

$$x_3 \pm x_0 = \eta_2 \frac{r}{r_+} e^{\pm r_+ \phi}.$$

r lives in the range (r_+, ∞) in regions 1 and 3 and $(0, r_+)$ in region 2. The BTZ identification in these coordinates is

$$\text{regions 1,2:} \quad (t, \phi, r) \cong (t, \phi + 2\pi, r),$$

$$\qquad\qquad\qquad\qquad (2.8)$$

$$\text{region 3:} \quad (t, \phi, r) \cong (t + 2\pi, \phi, r).$$

The metric is

$$ds^2 = -(r^2 - r_+^2)dt^2 + \frac{dr^2}{r^2 - r_+^2} + r^2 d\phi^2. \qquad (2.9)$$

In string theory there is also a nonvanishing B field, but we will not need its explicit form.

Noting that t is a timelike coordinate in region 3, we see that the BTZ identification (2.8) gives rise to closed timelike
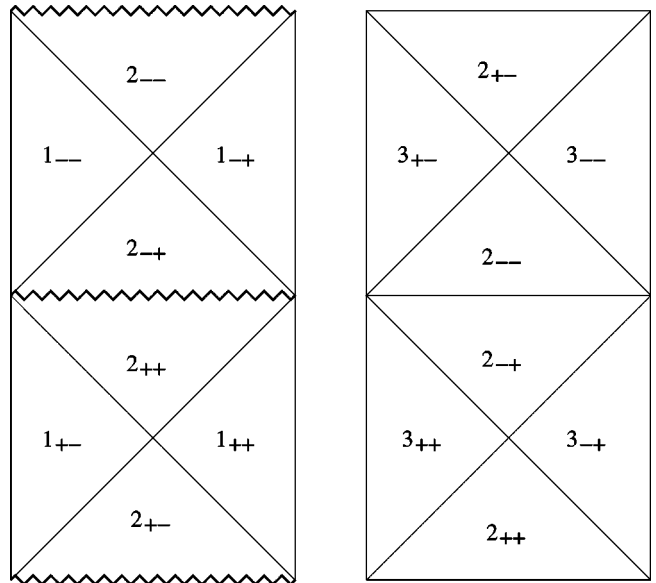

FIG. 1. Two orthogonal cross sections of the AdS_3 cylinder, with BTZ coordinate patches indicated. Both diagrams should be extended periodically in the vertical direction.

curves in this region. The desire to avoid these motivated the proposal to truncate the geometry at the singularity [30]. One goal of the present work is to examine whether such a truncation actually occurs in the context of string theory and the AdS/CFT correspondence.

To get a picture of the global structure, it is helpful to display two orthogonal cross sections of the original AdS_3 cylinder in Fig. 1, with the various coordinate regions indicated. Important for us is the fact that each component of regions 1 and 3 has a distinct boundary. One might then expect there to be distinct CFT's living on each boundary component; we will see in Sec. VII that the actual situation is more subtle.

B. Propagators and divergences

AdS/CFT correlation functions on the bulk side are constructed out of bulk-boundary and bulk-bulk propagators. The BTZ versions of these propagators can be obtained from their AdS_3 cousins by the method of images [34]. For the bulk-boundary propagator we need to specify a "source" point b on the boundary, and a "sink" point x in the bulk. In BTZ coordinates, the form of the propagator changes as we move the source and sink points from one region to another. For a minimally coupled scalar of mass m, the bulk-boundary propagator for both source and sink in region 1_{++} is, up to normalization,

$$K^{(1_{++}1_{++})}(x,b') = \sum_{n=-\infty}^{\infty} \frac{1}{\left[-\sqrt{\frac{r^2-r_+^2}{r_+^2}}\cosh(r_+\Delta t) + \frac{r}{r_+}\cosh r_+(\Delta\phi+2\pi n)\right]^{2h_+}}. \tag{2.10}$$

Here $\Delta t = t - t'$, and similarly for $\Delta\phi$. A bulk scalar of mass m corresponds to a boundary operator of conformal dimension $2h_+ = 1 + \sqrt{1+m^2}$. Although written for region 1_{++}, in fact K is always given by Eq. (2.10) whenever the source and sink point are in the same region. Equation (2.10) diverges when the bulk and boundary points are lightlike separated, and so an $i\epsilon$ prescription is required. We will see how to obtain the correct $i\epsilon$ prescription when we discuss the continuation from Euclidean signature.

To move the sink point to another region, we can analytically continue the propagator. For instance, by examining Eq. (2.5), we see that to move the sink point to 1_{+-} we should make the replacement $t \to t - i\pi/r_+$. Note that the imaginary shift is half the inverse Hawking temperature

$$\beta = 1/T_H = 2\pi/r_+. \tag{2.11}$$

Making this replacement, the bulk-boundary propagator becomes

$$K^{(1_{+-}1_{++})}(x,b') = \sum_{n=-\infty}^{\infty} \frac{1}{\left[\sqrt{\frac{r^2-r_+^2}{r_+^2}}\cosh(r_+\Delta t) + \frac{r}{r_+}\cosh r_+(\Delta\phi+2\pi n)\right]^{2h_+}}. \tag{2.12}$$

This propagator is nonsingular, reflecting the fact that 1_{++} and 1_{+-} are spacelike separated.

To investigate the behavior of the propagator near the BTZ singularity we now move the sink point to 2_{++},

$$K^{(2_{++}1_{++})}(x,b') = \sum_{n=-\infty}^{\infty} \frac{1}{\left[-\sqrt{\frac{r_+^2-r^2}{r_+^2}}\sinh(r_+\Delta t) + \frac{r}{r_+}\cosh r_+(\Delta\phi+2\pi n)\right]^{2h_+}}. \tag{2.13}$$

This is singular at $r=0$, since the summation then acts on an n independent quantity. By estimating the number of term in the sum which contribute as $r \to 0$, we find that near the singularity

$$K^{(2_{++}1_{++})} \sim f(\Delta t)\ln r. \tag{2.14}$$

The same divergence applies when we approach the singularity from other regions. The bulk-bulk propagators also diverge logarithmically for the same reason.

Let us first be very naive and see why we might expect divergent amplitudes to arise. A typical supergravity calculation of an AdS/CFT amplitude involves a Feynman diagram composed of propagators and vertices, and an integration over the positions of the vertices. Divergences can therefore arise from the region of integration involving some number of vertices approaching the BTZ singularity. In fact, since the integration measure is $\int dt\, d\phi\, dr\, r$, nonderivative couplings will yield finite amplitudes after integration. However, an

interaction with a sufficient number of derivatives will lead to a divergent integral. The divergences arise due to an infinite blueshifting at the singularity, as in recent examples of time dependent orbifolds of Minkowski space. For the Milne singularity, divergences in string amplitudes are studied in Ref. [32]. In Sec. VII we will see how the AdS/CFT correspondence handles these divergences.

III. PROBING THE SINGULARITY WITH SPACELIKE GEODESICS

From our knowledge of the bulk-boundary propagator in the various regions, we can make a few preliminary comments about how AdS/CFT correlators might probe the singularity. We will see later that the situation is considerably more subtle than these considerations suggest. As a specific example, consider a two point function with one operator inserted on the boundary of 1_{++} and another on the boundary of 1_{+-}. According to the standard AdS/CFT rules, Eq. (2.12) leads to the two point function [22]

$$\langle \mathcal{O}_{1_{+-}} \mathcal{O}_{1_{++}} \rangle$$

$$= \sum_{n=-\infty}^{\infty} [\cosh(r_+ \Delta t) + \cosh r_+ (\Delta \phi + 2\pi n)]^{-2h_+}. \tag{3.1}$$

Given the BTZ causal structure, correlators involving operators in both 1_{++} and 1_{+-} might be expected to probe physics behind the horizon and in particular near the singularity. We can make this expectation a bit more precise by using the WKB approximation to see which spacetime geodesics contribute to Eq. (3.1). Consider for simplicity the two-point function with $\Delta \phi = 0$. The equation for a spacelike geodesic is

$$\frac{\dot{r}^2}{r^2 - r_+^2} - \frac{E^2}{r^2 - r_+^2} = 1, \tag{3.2}$$

where $\dot{}$ denotes a proper time derivative and E is the conserved energy $E = (r^2 - r_+^2)\dot{t}$. Integrating we find

$$r(\tau) = \begin{cases} \pm \sqrt{E^2 - r_+^2} \sinh(\tau - \tau_0), & E^2 > r_+^2, \\ \pm \sqrt{r_+^2 - E^2} \cosh(\tau - \tau_0), & E^2 < r_+^2. \end{cases} \tag{3.3}$$

For $E^2 > r_+^2$ the geodesics cross the singularity at $r = 0$, and so we focus on the $E^2 < r_+^2$ case and choose the $+$ sign. The distance of closest approach to the singularity is

$$r_{\min} = \sqrt{r_+^2 - E^2}. \tag{3.4}$$

We want to relate E to the values of the boundary time coordinates. Integrating the equations for t gives

$$\Delta t = t(\infty) - t(-\infty) = -\frac{i\pi}{r_+} + \frac{1}{r_+} \ln \left\{ \frac{1 + \dfrac{E}{r_+}}{1 - \dfrac{E}{r_+}} \right\}. \tag{3.5}$$

The imaginary part $-i\beta/2$ is the correct jump when going between 1_{++} and 1_{+-}. The real part Δt_r is related to $r_{\min}$ by

$$r_{\min} = \frac{r_+}{\cosh\left(\dfrac{r_+ \Delta t_r}{2}\right)}. \tag{3.6}$$

In our conventions time runs backward in 1_{+-}, which is consistent with the fact that $r_{\min}$ is invariant under simultaneous time translations in the initial and final times.

The WKB approximation to the two-point function is given by e^{-S}, where S is the action of the spacelike geodesic passing between the two boundary points. This action is divergent; using a large r cutoff the regularized action is

$$S = m\Delta\tau = 2m \ln \left(\frac{2r_c \cosh\left(\dfrac{r_+ \Delta t_r}{2}\right)}{r_+} \right). \tag{3.7}$$

We define a renormalized action S_{ren} by subtracting $2m \ln r_c$, since this term also arises in pure AdS$_3$. The WKB approximation to the two point function is then

$$e^{-S_{\text{ren}}} = \frac{C}{\left[\cosh\left(\dfrac{r_+ \Delta t_r}{2}\right) \right]^{2m}}. \tag{3.8}$$

When we recall that for large m, which is when the WKB approximation is accurate, $2h_+ = 1 + \sqrt{1 + m^2} \approx m$, we find that Eq. (3.8) agrees with the leading term in Eq. (3.1).

We can ask for the time scale at which the geodesic passes within a proper distance L_{Pl} of the singularity, which is when we could expect quantum effects to become important. Restoring the AdS$_3$ length scale, this is

$$\Delta t_{\text{sing}} \sim \frac{2L_{\text{AdS}}^2}{r_+} \ln \left(\frac{L_{\text{AdS}}}{L_{\text{Pl}}} \right). \tag{3.9}$$

Another important timescale was pointed out by Maldacena [22]. This is the time scale where large fluctuations in the geometry apparently become important. For sufficiently large time separation $\Delta t > \Delta t_{\text{fluc}}$ (3.8) is inconsistent with unitarity of the boundary theory, since the correlation should not drop below e^{-s}, where s is the entropy,

$$s = \frac{\pi r_+}{2L_{\text{Pl}}}. \tag{3.10}$$

This gives

$$\Delta t_{\text{fluc}} \sim \frac{\pi}{2} \frac{L_{\text{AdS}}}{mL_{\text{Pl}}}. \tag{3.11}$$

The time Δt_{fluc} marks the onset of fluctuations in the correlation function of size $\sim \exp(-s)$. A much longer time, the Poincaré recurrence time $\Delta t_{\text{recur}} \sim \exp(as)$ marks the onset of order one fluctuations [22,35]. From the bulk point of view, an indication of the time scale for fluctuations can be seen in the WKB approximation when we recall that we should really consider the sum of the actions of the geodesic and the background geometry. The action of the black hole is related to its free energy

$$S_{\text{BH}} = -(s - \beta M) = -\frac{\pi}{4} \frac{r_+}{L_{\text{Pl}}}. \tag{3.12}$$

On the other hand, recalling that pure AdS$_3$ has energy $M = -1/8L_{\text{Pl}}$, the action of thermal AdS$_3$ at inverse temperature β is

$$S_{\text{AdS}} = \beta M = -\frac{\pi}{4} \frac{L_{\text{AdS}}^2}{L_{\text{Pl}} r_+}. \tag{3.13}$$

So for $r_+ > L_{\text{AdS}}$ the black hole dominates the partition sum. However, this can be overcome by the positive action of the action for the spacelike geodesic. Indeed, the time scale for the geodesic action to become comparable to the black hole action recovers (up to a numerical factor) the result (3.11).

Comparing Eq. (3.9) with Eq. (3.11), we see that for $m \sim L_{\text{AdS}}$, $r_+ \sim L_{\text{AdS}} \gg L_{\text{Pl}}$, we have $\Delta t_{\text{fluc}} \gg \Delta t_{\text{sing}}$. Therefore, we might hope to use boundary correlators to probe the physics of the singularity before possible fluctuations in the whole geometry become important. This will turn out to be only indirectly the case.

IV. ANALYTIC CONTINUATION I: FINITENESS OF AMPLITUDES

The heuristic arguments just given are not sufficient to determine to what extent we can really probe the singularity. The divergences arising in time dependent orbifolds of Minkowski space have to do with interactions near the singularity. Similarly, in the BTZ case we need to go beyond the two-point function and include interactions in the bulk.

At our current level of understanding, string theory in Lorentzian AdS$_3$ or BTZ is defined by analytic continuation from Euclidean signature [36–38]. This is the approach we will follow; we will discuss later whether this procedure really captures all of the Lorentzian physics.

The Euclidean BTZ metric is given by the replacement $t = -i\tau$

$$ds^2 = (r^2 - r_+^2)d\tau^2 + \frac{dr^2}{r^2 - r_+^2} + r^2 d\phi^2, \tag{4.1}$$

with

$$\tau \cong \tau + \beta, \tag{4.2}$$

and β given by Eq. (2.11). The radial coordinate is now restricted to (r_+, ∞). Given the periodicity of τ and ϕ, Eq. (4.1) is topologically a solid torus. The boundary CFT therefore lives on a torus parametrized by τ and ϕ.

A Euclidean AdS/CFT n-point function is labeled by n points on the boundary torus $G_n(\tau_1, \phi_1, \ldots, \tau_n, \phi_n)$. The amplitudes are initially defined for real τ, or equivalently for pure imaginary t. To obtain Lorentzian amplitudes we need to perform an analytic continuation in t. Continuing a point to real t gives a point on a boundary component of Lorentzian BTZ, which we can take to be in 1_{++}. As we have already mentioned, to get from 1_{++} to 1_{+-} one takes $t \to t - i\beta/2$. So, starting from t on the imaginary axis we need the continuations

$$t \to \begin{cases} \text{real}, & 1_{++}, \\ \text{real} - i\beta/2, & 1_{+-}. \end{cases} \tag{4.3}$$

We will defer to later the question of continuing to other boundary components.

We now want to argue that the analytically continued amplitudes are finite. The argument can be made in terms of either the bulk or boundary descriptions. From the boundary point of view, since we know that our amplitudes correspond to those of a well behaved CFT on the boundary torus, we do not expect there to arise any unusual singularities in amplitudes even after analytic continuation. We expect correlation functions defined for real t to be analytic in t, order by order in the string loop counting parameter. This follows from a well behaved spectral decomposition (a natural expectation) or from the perturbative bulk correspondence. This analyticity implies that singularities will be at most complex codimension one. But the kind of singularities induced by effects such as Eq. (2.14) will in general be of real codimension 1.[3] Another way of saying this is that, as we review in the next section, Lorentzian amplitudes are manifestly regular and finite since they can be expressed as expectation values evaluated in the entangled state

$$|\Psi\rangle = \frac{1}{\sqrt{\mathcal{Z}}} \sum_n e^{-\beta E_n/2} |n\rangle \otimes |n\rangle, \tag{4.4}$$

where $|n\rangle$ is an energy eigenstate with energy E_n in the Hilbert space of the CFT and $\mathcal{Z}$ is the partition function.

From the bulk point of view, the basic point is that the Euclidean BTZ geometry is completely smooth, as usual for Euclidean black holes, since the region $r < r_+$ does not appear. Therefore, string theory or supergravity amplitudes computed in Euclidean signature will be finite, modulo the usual divergences that occur even for pure AdS$_3$, such as due to tachyons and so forth, and can be analytically continued to Lorentzian signature as above. One may think that there is a possibility that these amplitudes do not have good asymptotic expansions in the string coupling constant. This,

---

[3]The tree level Liu-Moore-Seiberg (LMS) amplitudes [8] have singularities only at complex codimension one, but higher orders are expected to be generically singular [13,14].

however, is not likely. Since the BTZ geometry is an orbifold of AdS$_3$, at the tree level, a correlation function in the former can be expressed as a sum over the corresponding correlation function in the latter under the action of the orbifold group. This sum is manifestly convergent [22]. Moreover, as we will see in the next section, correlation functions of operators on 1_{++} and 1_{+-} can be computed taking into account interactions taking place outside of the horizon only. Thus we do not expect divergences associated to the singularity to arise at higher loops either. Of course, field theoretic divergences could be rendered finite by stringy α' effects, but this seems unlikely, especially given the stringy divergences found in Ref. [8].

V. ANALYTIC CONTINUATION II: BOUNDARY THEORY

Analytic continuation from Euclidean signature yields finite amplitudes, and we now want to examine in more detail how this comes about. As we discussed previously, Lorentzian signature divergences seemingly arise from integrating an interaction vertex near the BTZ singularity. We will find two different interpretations, corresponding to two different contour deformations, for how the singularity is avoided. In the first, interactions only occur in regions 1_{++} and 1_{+-}, so that the region near the singularity never appears in the calculation. In the second interpretation the region near the singularity does appear, but the analytic continuation provides an $i\epsilon$ prescription which tells us how to go around the singularity in the complex plane.

It is useful to begin by reviewing the analytic continuation in the boundary theory, following the work of Niemi and Semenoff [39]. For simplicity, we consider a weakly interacting scalar field theory on the Euclidean torus. We consider the computation of Euclidean time ordered correlation functions

$$G_n(\tau_1,\phi_1,\ldots,\tau_n,\phi_n)$$
$$= \mathrm{Tr}\{e^{-\beta H}T[X(\tau_1,\phi_1),\ldots,X(\tau_n,\phi_n)]\}$$
$$= \int_{\mathrm{periodic}} \mathcal{D}X \, e^{-S} X(\tau_1,\phi_1),\ldots,X(\tau_n,\phi_n).$$

$$(5.1)$$

We imagine computing Feynman diagrams in position space, so we will have interaction vertices integrated over the Euclidean torus. A simple example is the lowest order three-point function in the presence of a λX^3 interaction,

$$G_3(\tau_1,\phi_1,\tau_2,\phi_2,\tau_3,\phi_3) \sim \lambda \int_0^\beta d\tau \int_0^{2\pi} d\phi \, G(\tau,\phi,\tau_1,\phi_1)$$
$$\times G(\tau,\phi,\tau_2,\phi_2) G(\tau,\phi,\tau_3,\phi_3).$$

$$(5.2)$$

Now relabel $\tau_i = it_i$ and $\tau = it$ and consider analytically continuing G_n to the real t_i axis. The point is that the propagators have singularities for lightlike separated arguments. The positions of these singularities in the complex t plane
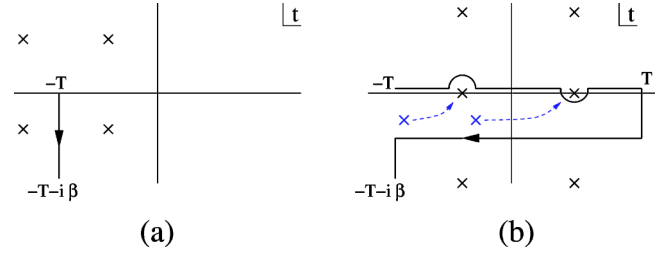

FIG. 2. Integration contours for evaluating correlation functions. Contour (a) defines a Euclidean amplitude; analytic continuation to real time gives (b).

will move around as we continue in t_i, and we have to deform the contour of integration so that no singularities cross the contour. Singularities occur for

$$t=t_i \pm (\phi-\phi_i-2\pi m)+in\beta, \quad n,m=\text{integer}. \quad (5.3)$$

The t contour of integration originally runs from 0 to $-i\beta$ along the imaginary axis. It is convenient to use translation invariance to instead take the contour to run from $-T$ to $-T-i\beta$ with T real and positive. The following analysis applies for any value of T, but we will eventually take $T \to \infty$ since this leads to the simplest real time interpretation.

So before doing any analytic continuation, Fig. 2(a) shows the integration contour and the locations of singularities in the integrand. Note that no matter how large T is, there are always singularities to the left of the contour due to the periodicity in ϕ.

We have only drawn the singularities due to a single propagator to avoid clutter. Now move t_i to the real axis. The locations of singularities move according to Eq. (5.3). Deforming the contour to avoid the singularities, we end up with the contour in Fig. 2(b). We are left with two segments parallel to the real axis, as well as two segments parallel to the imaginary axis. Singularities on the real axis are avoided by the usual prescription leading to the Feynman Green's function.

The result has a simple operator interpretation, which can be found by going through the usual steps relating path integral and operator expressions. Normally, we consider contours with just a single horizontal component, which leads to expectation values in the vacuum state. If we now add a second horizontal contour we get a second copy of the field theory, with expectation values again computed in the vacuum state. The Hilbert space of the full theory is then $\mathcal{H} \otimes \mathcal{H}$, where $\mathcal{H}$ is the Hilbert space of the field theory on the cylinder. Our contour also includes vertical segments which establish a correlation between the two sectors of the Hilbert space. In particular, the path integral along a vertical segment represents an insertion of the operator $e^{-\beta H/2}$, corresponding to an imaginary time translation by $\beta/2$. So instead of projecting onto the vacuum state of the tensor product theory, we have an entangled state with the entanglement given by the operator $e^{-\beta H/2}$.

More precisely, our result can be written in operator form as

$$G_n = \langle \Psi | T[X(t_1,\phi_1),\ldots,X(t_n,\phi_n)] | \Psi \rangle, \quad (5.4)$$
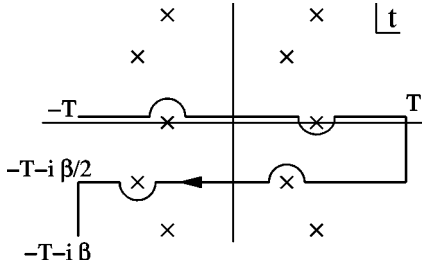
FIG. 3. Time integration contour for operators on both Lorentzian copies.

where $|\Psi\rangle$ is an entangled state in $\mathcal{H} \otimes \mathcal{H}$,

$$|\Psi\rangle = \frac{1}{\sqrt{\mathcal{Z}}} \sum_n e^{-\beta E_n/2} |n\rangle \otimes |n\rangle. \tag{5.5}$$

T in Eq. (5.4) now represents Lorentzian time ordering. Since we have continued to the real t axis, the X operators in Eq. (5.4) all represent operators in a single copy of the field theory, say the first. It is clear that we can then perform the trace over states in the second copy, and recover a thermal expectation value for operators in the first copy,

$$G_n = \mathrm{Tr}\{e^{-\beta H} T[X(t_1, \phi_1), \ldots, X(t_n, \phi_n)]\}. \tag{5.6}$$

It is straightforward to generalize the previous argument to the case where some operators are continued to $t = \mathrm{Re} -i\beta/2$. The resulting contour appears as in Fig. 3.

The expression (5.4) is unchanged, except that now whichever operators were taken to $t = \mathrm{Re} - i\beta/2$ now appear as operators in the second copy of the field theory. Finally, we can also consider continuing operators to the vertical segments of the final contour. This has the effect of replacing $e^{-\beta H/2}$ by a more general operator, and so corresponds to changing the state from Eq. (5.5) to something else.

Let us make a few comments about these results. First, although we only explicitly discussed the continuation of diagrams with a single vertex, the argument is easily generalized by considering each vertex in turn. Second, it is important to note that the continuation instructs us to integrate vertices over the entire contour, including the vertical segments. The presence of interactions on the vertical segments ensures that the energy eigenstates appearing in Eq. (5.5) are the correct energy eigenstates of the full interacting theory. Integrating only over the horizontal segments would yield energy eigenstates of the free theory.

As noted by Israel [25] shortly after Hawking's derivation of black hole radiance (and in the context of AdS/CFT in Refs. [22,26,27]), the fact that real time thermal correlators are naturally interpreted in terms of a tensor product of two field theories is directly analogous to the fact that constant time hypersurfaces in an eternal black hole geometry naturally consist of two components on either side of the horizon. In our notation, the two components correspond to 1_{++} and 1_{+-}. So the expectation that there should be two boundary theories associated with the two boundaries of 1_{++} and 1_{+-} is borne out by analytic continuation.
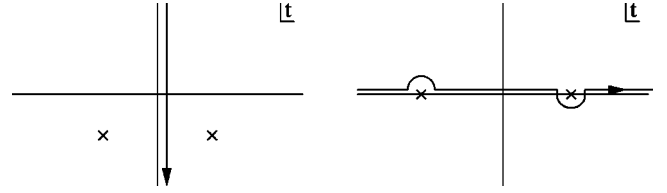

FIG. 4. Standard contour rotation defining amplitudes in Minkowski space.

VI. ANALYTIC CONTINUATION III: MINKOWSKI SPACE

There is some additional freedom to analytically continue bulk amplitudes corresponding to different choices of time coordinates. Different choices will lead to different Lorentzian interpretations of the same correlation functions. Before proceeding to the black hole case we will do a warmup example.

We start by computing Green's functions in flat Euclidean space

$$ds^2 = d\tau^2 + dx^2. \tag{6.1}$$

So, for example, the expression analogous to Eq. (5.2) is now

$$G_3(\tau_1, x_1, \tau_2, x_2, \tau_3, x_3) \sim \lambda \int_{-\infty}^{\infty} d\tau \int_{-\infty}^{\infty} dx \, G(\tau, x, \tau_1, x_1)$$
$$\times G(\tau, x, \tau_2, x_2) G(\tau, x, \tau_3, x_3). \tag{6.2}$$

The standard procedure is to continue in $t_i = -i\tau_i$ while rotating the time contour to the real t axis. An $i\epsilon$ prescription follows from taking the contour to be at a small angle with respect to the real axis, or equivalently, to go around the singularities as in Fig. 4.

The result is that we are to integrate vertices over Minkowski spacetime using the Lorentzian propagator

$$G_{\mathrm{Lor}}(t, x, t', \phi') = G(e^{i(\pi/2 - \epsilon)} t, x, e^{i(\pi/2 - \epsilon)} t', \phi'). \tag{6.3}$$

Since the Euclidean propagator is a function of $\sigma^2 = (\tau - \tau')^2 + (x - x')^2$, the rule to obtain the Lorentzian propagator is

$$\sigma^2 \to -(t - t')^2 + (x - x')^2 + i\epsilon. \tag{6.4}$$

We can alternatively analytically continue with respect to Rindler time. To do this we transform to polar coordinates

$$\tau = r \sin\theta, \quad x = r \cos\theta, \quad ds^2 = dr^2 + r^2 d\theta^2. \tag{6.5}$$

The Euclidean integration is now $\int_0^{\infty} dr \, r \int_0^{2\pi} d\theta$.

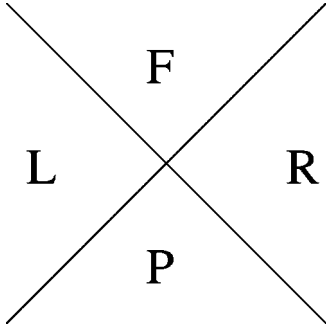Recall that Rindler coordinates cover Minkowski spacetime in four patches

FIG. 5. Rindler coordinate patches.

$$x \pm t = \begin{cases} re^{\pm\eta}, & R, \\ -re^{\pm\eta}, & L, \\ re^{\mp\eta}, & F, \\ -re^{\mp\eta}, & P, \end{cases} \qquad (6.6)$$

with metric

$$ds^2 = \begin{cases} -r^2\,d\eta^2 + dr^2, & R, L, \\ r^2\,d\eta^2 - dr^2, & F, P. \end{cases} \qquad (6.7)$$

Note that region L is obtained from region R by $\eta \to \eta - i\pi$. We will take $\eta = -i\theta$ to be the Rindler coordinate in region R (see Fig. 5).

Now, the geodesic distance expressed in terms of r and η is

$$\sigma^2 = r^2 + r'^2 - 2rr'\cosh(\eta - \eta'). \qquad (6.8)$$

Therefore, singularities in the complex η plane are located at

$$\eta = \eta_i + \frac{1}{2rr_i}\cosh^{-1}(r^2 + r_i^2) = \eta_i + 2\pi in + \pm\mathrm{Re}. \qquad (6.9)$$

With $\beta = 2\pi$, our integration contour in the η plane and the location of singularities are precisely the same as in our earlier discussion of continuing correlators on the Euclidean cylinder. Therefore, we can deform the contour as in Fig. 2 (with t replaced by η). The two horizontal segments now correspond to integration over region R and L. The appearance of a tensor product is now seen to be due to the fact that the $t=0$ Minkowski timeslice is a sum of $\eta = 0$ time slices in the right and left Rindler patches.

Green's function computed by continuation in either Minkowski or Rindler time should agree, and this indeed follows from the fact that the entangled state arising in the Rindler description

$$|\Psi\rangle = \frac{1}{\sqrt{\mathcal{Z}}} \sum_n e^{-\pi E_n} |n\rangle_R \otimes |n\rangle_L \qquad (6.10)$$

is equal to the usual Minkowski vacuum [40]. To see that the two states are the same, consider a path integral on the lower half Euclidean plane, with prescribed boundary conditions $\phi(x)$ on the real axis. This wave function $\Psi[\phi(x)]$ defines the Minkowski vacuum state. On the other hand, we can consider the Hilbert space of wave functions on half of the real axis, with a Rindler Hamiltonian H_R corresponding to rotations about the real axis. The path integral then becomes the transition amplitude $\langle\phi_L|e^{-\pi H_R}|\phi_R\rangle$, where $\phi_{L,R}$ are the boundary conditions $\phi(x)$ restricted to the left and right halves of the real axis. Inserting a complete set of eigenstates of H_R then leads to the equivalence of the two states.

So to summarize, Green's functions with arguments in regions R and L can be computed either in the usual fashion by integrating vertices over all of Minkowski space, or by just integrating over the R and L wedges with an entanglement given by Eq. (6.10). If we imagine first doing the integration over the vertical segments of the Rindler contour, this will result in wave functions inserted at $\eta = \pm\infty$. These wave functions provide the boundary conditions at the horizons which bound the two Rindler wedges. Equivalently, the wave functions can be thought of as providing the "missing" part of the integrand from not integrating over the F and P wedges.

VII. ANALYTIC CONTINUATION IV: BEHIND THE BLACK HOLE HORIZON

Now we are ready to discuss analytic continuation to compute correlation functions in the Lorentzian BTZ black hole.

A. BTZ coordinates

We first consider analytic continuation in BTZ coordinates (2.9). This is straightforward and follows closely our discussion of analytic continuation in Rindler time. Singularities in propagators, occurring, as always, for lightlike separation, are located in the complex time plane at

$$t = t' + \mathrm{Im}\,\beta \pm \mathrm{Re}. \qquad (7.1)$$

For instance, for the bulk-boundary propagator given in Eq. (2.10) the singularities are located at

$$t = t' + \mathrm{Im}\,\beta + \cosh^{-1}\left(\sqrt{\frac{r^2}{r^2 - r_+^2}}\cosh r_+(\Delta\phi + 2\pi n)\right). \qquad (7.2)$$

Euclidean AdS/CFT amplitudes are defined as

$$A_n(b_1', \ldots, b_n') = \left(\prod_{i=1}^{n} \int_0^{2\pi} d\phi_i \int_{r_+}^{\infty} dr_i\, r_i \int_C dt_i\right)$$
$$\times K(x_1, b_1')\cdots K(x_n, b_n')G_n(x_1, \ldots, x_n), \qquad (7.3)$$

where the n-point Greens function G_n represents the part of the amplitude corresponding to bulk-bulk propagators only. Equation (7.3) corresponds to nonderivative interactions, but the generalization is straightforward. The time integration contour C runs down along the imaginary axis from 0 to $-i\beta$. As before we use time translation invariance to shift the contour in the real direction by $-T$, where we eventually take $T \to \infty$.

Proceeding as in our other examples, we want to continue t_i' from the contour C to either $t_i' = \mathrm{Re}$ or $t_i' = \mathrm{Re} - i\beta/2$. Using the fact that all singularities are located as in Eq. (7.1), the contour should be deformed as in Figs. 2 and 3. The region of integration along the real time axis corresponds to 1_{++}. Continuing the coordinate in 1_{++} by $-i\beta/2$ takes us to region 1_{+-}, so the second horizontal time contour represents an integration of this region. The two vertical segments of the contour establish a correlation between states in the two regions. The entangled state is as in Eq. (5.5),

$$|\Psi\rangle = \frac{1}{\sqrt{\mathcal{Z}}} \sum_n e^{-\beta E_n/2} |n\rangle \otimes |n\rangle. \qquad (7.4)$$

By the same argument as in the Minkowski/Rindler example, this state is equivalent to the one defined by a path integral on the lower half portion of the Euclidean black hole—the Hartle-Hawking vacuum. We again remark that the fact that interaction vertices are to be included on the vertical segments of the contour ensures that the energy eigenstates appearing in Eq. (7.4) are those of the full interacting theory.

If we imagine first doing the integration over the vertical segments then this leaves us with correlated boundary conditions for the horizontal segments at large positive and negative BTZ time. In particular, it gives boundary conditions along the past and future horizons in regions 1_{++} and 1_{+-}. Since $t = +\infty$ corresponds to the future horizon in 1_{++} and the past horizon in 1_{+-}, boundary conditions on these two horizons are correlated by the rightmost vertical segment. And similarly for the leftmost vertical segment. The correlated boundary conditions are equivalent to computing expectation values in the state (7.4).

Starting from Euclidean propagators expressed in terms of Euclidean time τ, the arguments of the propagator can be taken to either 1_{++} or 1_{+-} by the replacements

$$\tau \rightarrow \begin{cases} e^{i(\pi/2-\epsilon)}t, & 1_{++} \\ e^{-i(\pi/2-\epsilon)}t + \beta/2, & 1_{+-}. \end{cases} \qquad (7.5)$$

For instance, the bulk-boundary propagator with both arguments in 1_{++} is

$$K^{(1_{++}1_{++})}(x,b') = \sum_{n=-\infty}^{\infty} \frac{1}{\left[-\sqrt{\frac{r^2-r_+^2}{r_+^2}}\cosh(r_+\Delta t) + \frac{r}{r_+}\cosh r_+(\Delta\phi + 2\pi n) + i\epsilon\Delta t \sinh(r_+\Delta t) \right]^{2h_+}}. \qquad (7.6)$$

Propagators with arguments in distinct regions do not need an $i\epsilon$ prescription, since such propagators are nonsingular due to the spacelike separation of points in 1_{++} and 1_{+-}.

The Lorentzian prescription obtained by analytic continuation in BTZ time is therefore to integrate vertices over regions 1_{++} and 1_{+-} with propagators given by the rule (7.5). Furthermore, we should also integrate over the imaginary time segments shown in Figs. 2 and 3, or equivalently impose correlated boundary conditions on the horizons bounding the two regions. This prescription has also appeared in the recent work [41].

With this prescription, the regions of the BTZ spacetime near the singularities do not appear in the computation, and so it is clear that there are no divergences from infinite blueshifts. All knowledge about physics in other regions besides 1_{++} and 1_{+-} is contained in the Hartle-Hawking wave function.

This approach gives a satisfactory description involving only regions 1_{++} and 1_{+-}, but it is natural to expect that there will exist alternative descriptions in which other regions of the BTZ spacetime play a role. Here an analogy with our Minkowski spacetime example is helpful. We saw that we would analytically continue with respect to either Rindler or Minkowski time. In the Rindler case, which is analogous to using BTZ coordinates, only the left and right wedges appeared in the final result. On the other hand, the full spacetime appears in the Minkowski case, and so we would now like to find the analogous continuation for the BTZ spacetime. This is achieved by working in Kruskal coordinates, as we now discuss.

B. Kruskal coordinates

Lorentzian Kruskal coordinates are defined as

$$x_1 = \frac{1+X^2-T^2}{1-X^2+T^2}\cosh(r_+\phi),$$

$$x_2 = \frac{1+X^2-T^2}{1-X^2+T^2}\sinh(r_+\phi),$$

$$x_3 = \frac{2X}{1-X^2+T^2},$$

$$x_0 = \frac{2T}{1-X^2+T^2}. \qquad (7.7)$$

Note that $x_1^2 - x_2^2 \geq 0$, as given in Eq. (2.4), the coordinates do not cover the regions 3 containing the closed timelike curves. They do cover all of regions 1 and 2. More precisely, they cover all of regions 1 and 2 displayed in Fig. 1, but not those obtained by periodically extending the figures in the vertical direction. The AdS boundaries are at $X^2-T^2=1$, and we approach either the boundaries of $1_{+\pm}$ or $1_{\pm-}$ depending on

whether we approach $X^2 - T^2 - 1 = 0$ from negative or positive values. The BTZ singularities are located at $X^2 - T^2 = -1$. The metric is

$$ds^2 = \frac{4}{(1 - X^2 + T^2)^2} \left[-dT^2 + dX^2 \right.$$
$$\left. + \frac{r_+^2}{4} (1 + X^2 - T^2)^2 \, d\phi^2 \right]. \tag{7.8}$$

For reference, the relation with BTZ coordinates in 1_{++} is

$$r = \frac{1 + X^2 - T^2}{1 - X^2 + T^2} r_+, \quad \cosh(r_+ t) = \frac{X}{\sqrt{X^2 - T^2}}, \quad \phi = \phi. \tag{7.9}$$

The Euclidean signature metric is

$$ds^2 = \frac{4}{(1 - X^2 - \tau^2)^2} \left[d\tau^2 + dX^2 + \frac{r_+^2}{4} (1 + X^2 + \tau^2)^2 \, d\phi^2 \right]. \tag{7.10}$$

The Euclidean manifold is given by the region $0 \leq X^2 + \tau^2 \leq 1$. This metric is nonsingular since the proper length of the ϕ orbit cannot shrink to zero. The metric near where the denominator vanishes is that of AdS in Euclidean Poincaré coordinates. The boundary of the space is $X^2 + \tau^2 = 1$, giving a torus.

Euclidean AdS/CFT amplitudes are now obtained by integrating vertices over the Euclidean manifold. However, analytic continuation to Lorentzian signature is somewhat inconvenient because of the constraint $0 \leq X^2 + \tau^2 \leq 1$ on the integration domain. Since the range of the X integration depends on τ, one finds a complicated analytic structure for the τ integrand. Instead, it would be much more convenient if we could extend the domain to the full (X, τ) plane. This can be achieved as follows.

We first observe that the metric is invariant under the *antipodal* map defined as $x \to x_A = -x$, where $x = (x_1, x_2, x_3, x_4)$. From Eq. (7.7) with $T = -i\tau$ we see that in Kruskal coordinates the antipodal map becomes

$$X \to \frac{X}{X^2 + \tau^2}, \quad \tau \to \frac{\tau}{X^2 + \tau^2}. \tag{7.11}$$

It follows that the region $X^2 + \tau^2 \geq 1$ describes a second copy of Euclidean BTZ, so if we extend our integration domain to the full (X, τ) cylinder we will be integrating over two copies of Euclidean BTZ. It is convenient to do this, and then divide by an appropriate factor at the end of the calculation.

To see how this works in more detail, we first observe that under the antipodal map (7.11) Euclidean propagators transform as $G \to (-1)^{2h_+} G$, where the phase depends on how we choose to go around the branch cut. For example this transformation law follows immediately for the Euclidean bulk-boundary propagator from its form

$$K(x, b') = \sum_{n=-\infty}^{\infty} \frac{(1 - X^2 - \tau^2)^{2h_+}}{[2XX' + 2\tau\tau' - (1 + X^2 + \tau^2)\cosh r_+ (\Delta\phi + 2\pi n)]^{2h_+}}. \tag{7.12}$$

This same transformation law holds for bulk-bulk Euclidean propagators [42,43]. Therefore, the effect of extending the integration with respect to a given vertex to an integration over the full (X, τ) plane is to multiply the original result by the coefficient

$$1 + \prod_i (-1)^{2h_{+,i}}, \tag{7.13}$$

where the product over i is a product over propagators attached to the vertex in question. To reproduce the original result, we should divide by the factor (7.13) after extending each integration to the two copies of Euclidean BTZ. In the supergravity limit, in which we are working in this paper, $\Sigma_i 2h_{+,i}$ for is always an integer, and the factor (7.13) is either 2 or 0. If it is 2, we just have to multiply the factor 1/2 to each vertex after integrating it over the two copies. On the other hand, if the factor (7.13) is zero, it means that the contributions from the two copies cancel with each other. The method of doubling the integration region is then not simply applicable in such a case, and a subtler analysis is

required. Of course for many reasons it would be desirable to find a way to carry out the analytic continuation directly for a single copy of the Euclidean BTZ with the constraint $X^2 + \tau^2 \leq 1$. In the following, we will consider the case when $\Sigma_i 2h_{+,i}$ is an even integer.

Now we proceed to analytically continue the Kruskal time arguments of our Euclidean amplitudes. The first step, as always, is to locate the singularities in the complex T plane. There are two kinds of singularities: those from the BTZ singularity and those from lightlike separation. The BTZ singularities are located on the real T axis at $T = \pm \sqrt{1 + X^2}$. Lightlike singularities in a propagator $G(x, x')$ occur when the geodesic distance vanishes, $\sigma^2(x, x') = 0$. Examining the geodesic distance $\sigma^2 = (\Delta x_0)^2 + (\Delta x_1)^2 - (\Delta x_2)^2 - (\Delta x_3)^2$ in the coordinates (7.7), we find that with T' on the imaginary axis there are two singularities in the complex T plane, to the left and right of the imaginary T axis. Therefore, before doing any analytic continuation, the singularity structure is as in Fig. 6(a). Now when we continue T' to the real axis, the singularities also migrate to the real T axis. The contour deformation is therefore similar to that in Minkowski space with Minkowski time, and we obtain the contour in Fig. 6(b).

The novel feature is that the continuation tells us how to integrate over both the BTZ singularities as well as the usual lightcone singularities.

Our final result is that we are to integrate over all of regions 1 and 2 of Lorentzian BTZ in Fig. 1, corresponding to the full (X,T) plane. With propagators obtained from Euclidean signature by the substitution $\tau = e^{i(\pi/2 - \epsilon)}T$. For instance, the Lorentzian bulk-boundary propagator is

$$K(x,b') = \sum_{n=-\infty}^{\infty} \frac{(1 - X^2 + T^2 - i\epsilon)^{2h_+}}{[2XX' - 2(1 - i\epsilon)TT' - (1 + X^2 - T^2 + i\epsilon)\cosh r_+ (\Delta\phi + 2\pi n)]^{2h_+}}. \tag{7.14}$$

Note that the integral domain is over the eight regions in the left side of Fig. 1—four regions between the past and the future singularities, and four more beyond the future singularity. We also have to remember that, since we started with two copies of Euclidean BTZ related to each other by the antipodal map (7.11), we needed to divide the amplitude by the factor 2. (We are assuming that $\Sigma_i 2h_{+,i}$ is an even integer.)

The antipodal transformation

$$X \to \frac{X}{X^2 - T^2}, \quad T \to \frac{T}{X^2 - T^2}, \tag{7.15}$$

maps the regions 1_{--} and 1_{-+}, which are beyond the future singularity, to the regions 1_{++} and 1_{+-}. Under this map, the propagator transforms as $G \to (-1)^{2h_+}G$. Therefore, rather than integrating over all the four regions $1_{\pm\pm}$, we can restrict the integral to the two regions 1_{++} and 1_{+-} and multiply the factor 2. This cancels the factor 1/2 we introduced earlier to extend the integration to the double of Euclidean BTZ. Thus the net result is that we integrate over the regions 1_{++} and 1_{+-} with the standard propagators as in Eq. (7.14). This result is reasonable since the boundaries of these two regions are identified with the $(1+1)$-dimensional spaces for the boundary CFT at finite temperature, as discussed in Sec. V [22]. If the regions 1_{--} and 1_{-+} were included, we would have had to impose boundary conditions for these regions and the question would have arisen whether there are additional boundary CFT's for these.

The situation is more subtle when the integral runs over regions of type 2. The antipodal transformation maps 2_{--} and 2_{-+} to 2_{++} and 2_{+-}, respectively. Under this, the propagator transforms as $G \to (-1)^{2h_+}G^*$, where the complex conjugation means that we are using the opposite of the standard $i\epsilon$ prescription. For the bulk-boundary propagator, we can see this directly by acting Eq. (7.15) on Eq. (7.14), but it is also true for the boundary-boundary propagator. Thus, if we want to restrict the integral region to be over 2_{++} and 2_{+-}, which are between the past and the future singularities in Fig. 1, we need to average over the two opposite $i\epsilon$ prescriptions in an appropriate way. We will see that this is closely related to the cancellation of divergences at these singularities.

To summarize, the analytic continuation to the Lorentzian BTZ using the Kruskal coordinates shows that amplitudes are expressed in terms of integrals of interaction points over the regions 1 and 2 between the past and the future singularities. For propagators in the region 1, we use the standard $i\epsilon$ prescription. On the other hand, for propagators ending in the region 2, we need to take an appropriate average over signs of $i\epsilon$.

C. Integrating over the singularities

The divergence of the propagator at the BTZ singularity has been rendered finite by the $i\epsilon$ prescription, since $1 + X^2 - T^2 + i\epsilon$ is nonvanishing on the real T axis. Instead of the divergent behavior (2.14), we now have near the singularities

$$K \sim f(X,T)\ln(1 + X^2 - T^2 + i\epsilon) \sim f(\Delta t)\ln(r + \pm i\epsilon). \tag{7.16}$$

The sign of $i\epsilon$ appearing in the last term depends on from which BTZ region we approach the singularity. A naive $i\epsilon$ prescription would consist of adding a small imaginary part to BTZ time and using the resulting propagator to integrate near the singularity. This procedure leads to the divergent propagator of Eq. (2.14) and to divergent amplitudes upon integration over the singularity. But now we see that the correct $i\epsilon$ prescription, written in terms of BTZ coordinates, adds an imaginary part to both r and t. Adding an imaginary part to r lets us define the amplitudes by integrating around the singularities in the complex plane. Analytic continuation has also been used previously (though not derived from a consistent starting point) in the context of quantum field theory near cosmological singularities, e.g., Ref. [44].

Let us examine the integration over the singularities in more detail. There are two BTZ singularities—past and future with respect to 1_{++} and 1_{+-}—located at $T =$
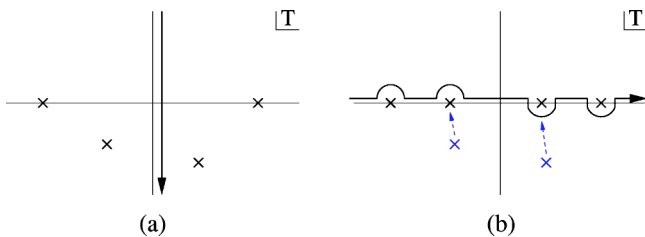

FIG. 6. Integration contours in the Kruskal time plane. In the left hand figure, singularities on the real axis are due to the BTZ singularity; those off the real axis are lightcone singularities.

$\pm\sqrt{1+X^2}$. Expressed in terms of BTZ coordinates, the metric near either of the singularities is

$$ds^2 = r_+^2\, dt^2 - \frac{dr^2}{r_+^2} + r^2\, d\phi^2 \qquad (7.17)$$

and the propagators behave as in Eq. (7.16). Examining Eq. (7.9), we see that, since our integration should extend over both sides of the singularities (if we do not identify the integration regions using the antipodal map), in BTZ coordinates we should integrate over both positive and negative r. Positive and negative r correspond to the past and future cones of the Milne universe. Note that we do not integrate over the left and right cones of Milne, since these correspond to regions of type 3, and these are not covered by the Kruskal coordinates.

We first consider the future singularity. Approaching the singularity from 2_{++} we have the relation [compare Eqs. (2.6) and (7.7)]

$$r \sim \frac{1 + X^2 - T^2}{2}. \qquad (7.18)$$

Therefore, propagators will diverge as $\ln(r+i\epsilon)$. If we take a generic derivative interaction, then the integration of a vertex near the singularity will include a piece

$$\int_{-r_c}^{r_c} dr\, \frac{\ln^p(r+i\epsilon)}{(r+i\epsilon)^q}, \qquad (7.19)$$

where r_c is the radius where the propagators start to differ from their leading behavior. As $\epsilon \to 0$, Eq. (7.19) gives a finite, but generically complex, result.

It is important that the imaginary parts arising from integration over the two singularities combine in a manner consistent with Hermiticity in the boundary CFT. Without checking this explicitly it is clear that this must come about, since our bulk amplitude is mathematically equivalent to the analytic continuation of the boundary CFT amplitude. But to illustrate the point we can make a simple check. Consider a boundary correlation function for Hermitian operators $\mathcal{O}_i(0,\phi)$ evaluated at $t=0$ on the boundary cylinder. Since the boundary theory is a tensor product, these operators can be associated with either of the CFTs defined on 1_{++} or 1_{+-}. Such a correlation function should be real, since all operators are spacelike separated and hence commute. When we compute the amplitude in the bulk we pick up imaginary parts from integrating over the BTZ singularities. But due to the relation $G \to (-1)^{2h_+} G^*$ under the antipodal transformation in the region 2, the imaginary parts cancel between the singularities, and the result is purely real as expected.

We have found that correlation functions computed in the BTZ black hole are free from divergences and unphysical imaginary parts because of the cancellation of effects at the past and future singularities. This nonlocal cancellation mechanism may seem surprising since it contradicts naive intuition that says that points closer to a singularity should feel much more of its effect. More quantitatively, in flat space a correlator falls similar to some power of the distance and so if the two singularities are far away the interaction points near the past singularity should make a much smaller effect than the ones near the future singularity. What makes a difference here is the asymptotically AdS boundary condition of the BTZ black hole, which lets geodesics reflect off the boundary and be refocused on future points. This makes it impossible to effectively separate the two singularities.

D. Defining scattering through the singularity

An extremely interesting question concerns the existence and behavior of scattering amplitudes for processes where particles "pass through" the singularity. This is the situation studied in Refs. [4,6–14,32]. The conclusion of this work, Ref. [8] in particular, is that such scattering amplitudes are badly behaved in string perturbation theory.

We might suppose that we could study such phenomena using the techniques discussed earlier. In particular we could study BTZ amplitudes with operators on the boundary of regions 1_{-+} and 1_{--} as well as 1_{++} and 1_{+-}. Any particle path between operators on boundaries above and below the singularity will have to pass through the singularity.

Formally we can calculate amplitudes like this by analytic continuation [31]. From Eq. (2.5) we see that we can "move" an operator from region 1_{++} to 1_{-+} by analytically continuing in ϕ, much as in Eq. (7.9):

$$\phi \to \begin{cases} [0,2\pi], & 1_{++}, \\ [0,2\pi] - i\beta/2, & 1_{-+}. \end{cases} \qquad (7.20)$$

The same continuation moves an operator from region 1_{+-} to region 1_{--}.

As we argued earlier, because the amplitudes we discuss are analytic in t and ϕ we do not expect singular behavior for generic operator locations on the boundary of 1_{-+} or 1_{--}. This seems to lead to a conflict with the singular behavior found in the references cited above. It also conflicts with a naive assumption that an analytic continuation for interaction point integrations on a purely real Lorentzian slice of the BTZ space as in Sec. VII exists for such boundary operator locations. If this were the case the $i\epsilon$ singularities would pinch the contour at the BTZ singularity and make the integrated amplitudes infinite in general.

One possible resolution concerns the boundary conformal field theory we might expect to find on the boundary of 1_{-+} or 1_{--}. The angular momentum operator that generates translations of ϕ has spectrum unbounded above and below. So the sum over conformal field theory states is at best conditionally convergent. This suggests that correlation functions might not be derivable directly from an operator formalism. But this does not resolve the above conflict because the analytically continued amplitudes might well define a consistent bulk theory by themselves, without a boundary field theory interpretation.

We believe the resolution to this problem lies in an obstruction to performing the analytic continuation of a boundary point into region 1_{-+} or 1_{--} with physical contours for the interaction points. We do not have a proof that such an obstruction always exists but all our attempts have encountered the same general problem.

This problem is illustrated by the following example. We work in BTZ coordinates and try to continue points to both 1_{++} and 1_{-+}. 1_{++} corresponds to Re t and Re ϕ; 1_{-+} corresponds to Re t and $\phi = \text{Re} - i\beta/2$. Now, start from the Euclidean contour and first continue to the Re t axis for all points. We can take the contour to have three segments: (1) go from $-T$ to $+T$ along the real axis, avoiding the singularities in the way which gives the Feynman propagator; (2) go from $+T$ to $-T$ along the real axis and underneath the singularities; (3) go from $-T$ to $-T-i\beta$. Now we would like to continue some of the boundary points to $\phi = \text{Re} - i\beta/2$ while also moving the ϕ contour of segment (2) down by $-i\beta/2$. This cannot be done since the ϕ contour is pinched. In particular, with the time argument given by segment (2), singularities along this segment occur at

$$-\sqrt{\frac{r^2 - r_+^2}{r_+^2}} \cosh r_+(\Delta t - i\epsilon) + \frac{r}{r_+} \cosh r_+(\Delta \phi + 2\pi n) = 0.$$

(7.21)

Expanding out the first cosh to first order in ϵ, we see that the imaginary part of $\Delta \phi$ changes sign depending on the sign of Δt. In general, both signs of Δt occur, so we will find singularities just above the real ϕ axis and just below—the contour is pinched. This prevents us from moving the ϕ contour downwards, unless we "drag" along some extra segment attached to the singularities. Other attempts result in the same pinching of the ϕ contour.

This obstruction prevents us from obtaining a simple picture of the Lorentzian signature amplitudes as integrals over the interaction point locations on a real section of the complexified BTZ space. This removes the conflict with other approaches that study that formulate the problem on this purely real section. But it also means that the techniques we have developed do not as yet resolve the issues raised in previous work.

E. Remarks

We have seen that a fixed Feynman diagram for correlators of boundary operators in the BTZ geometry can be understood in two different ways. First, as a Feynman diagram in which the locations of the interaction vertices are restricted to the regions outside the horizon. This is the "Rindler" type description. Second, as a diagram in which the locations are integrated over the full region covered by Kruskal coordinates, including regions behind the horizon and on both sides of the singularities. This is the "Minkowski" type description. This identification suggests that certain things about physics behind the horizon can be learned from data located outside the horizon. This idea is reminiscent of black hole complementarity.

In the second description, we integrate over interaction points inside of the horizon as well as outside. Divergences and unphysical imaginary parts, which could have appeared from an integral near a singularity (and which do appear in similar computations in the Milne universe [32]), are cancelled between the past and future singularities, at least in one case. At first glance this appears to be disturbingly nonlocal. But the singularities of eternal AdS-Schwarzschild black holes are never extremely far apart. Their maximum separation is of order the AdS radius, no matter how large the mass. The shortest distance simple boundary correlators can resolve is also AdS scale. To observe the isolated, uncancelled singular behavior of one singularity we would have to use probes sensitive to local bulk physics. We expect local correlators of bulk supergravity fields to show such singular behavior.[4] Extracting such local bulk physics from the boundary theory is a notoriously difficult problem. Perhaps the very complicated boundary operators necessary to localize quantities in the bulk will allow the well behaved boundary theory to display apparently singular bulk behavior.

The factor (7.13) that each Feynman diagram acquires under Kruskal analytic continuation starting with two copies of Euclidean BTZ black holes is a major shortcoming of our approach. In the supergravity limit, the factor is either 2 or 0 for each interaction vertex, and we were able to find a way to perform the analytic continuation in the Kruskal coordinates when it is 2. More generally, the factor is a complex-valued function of mass. The factor cancels out if the interaction point is in region 1, but it gives rise to a combination of G and G^* with complex coefficients in region 2. The mass dependence of these coefficients makes it difficult to perform the analytic continuation in the full string theory, though in that case we also need to discuss effects due to twisted sectors, etc. It is desirable to find a way to perform the analytic continuation starting with a single copy of Euclidean BTZ.

Our conclusions do not lean heavily on being in three spacetime dimensions, and one could extend our arguments to AdS black holes in other dimensions. Actually, much of what we say—minus the CFT interpretation—could also be said for the four-dimensional Schwarzschild solution. Green's functions defined in Euclidean signature can be analytically continued to Lorentzian signature, and in Kruskal coordinates will naturally lead to an integration over the black hole singularities.[5] One difference is that the Schwarzschild solution is only an approximate solution of string theory, and so the accuracy of the analytic continuation procedure needs more careful justification. In conclusion, our work illustrates the power of using analytic continuation to define otherwise divergent Lorentzian amplitudes, displaying a complementary correspondence between inside and outside the horizon phenomena in the process.

---

[4]Of course such quantities are not gauge invariant, but they may well be illustrative. In the $2+1$ BTZ situation the simplicity of the geometry allows cancellations to occur even for bulk correlators. This follows from the antipodal symmetry of bulk-bulk propagators.

[5]A path integral representation for the propagator was discussed from this point of view in Ref. [45].

[1] L. J. Dixon, J. A. Harvey, C. Vafa, and E. Witten, Nucl. Phys. **B261**, 678 (1985).

[2] A. Strominger, Nucl. Phys. **B451**, 96 (1995).

[3] C. V. Johnson, A. W. Peet, and J. Polchinski, Phys. Rev. D **61**, 086001 (2000).

[4] V. Balasubramanian, S. F. Hassan, E. Keski-Vakkuri, and A. Naqvi, Phys. Rev. D **67**, 026003 (2003).

[5] L. Cornalba and M. S. Costa, Phys. Rev. D **66**, 066001 (2002).

[6] N. A. Nekrasov, hep-th/0203112.

[7] J. Simon, J. High Energy Phys. **06**, 001 (2002).

[8] H. Liu, G. Moore, and N. Seiberg, J. High Energy Phys. **06**, 045 (2002); **10**, 031 (2002).

[9] S. Elitzur, A. Giveon, D. Kutasov, and E. Rabinovici, J. High Energy Phys. **06**, 017 (2002).

[10] L. Cornalba, M. S. Costa, and C. Kounnas, Nucl. Phys. **B637**, 378 (2002).

[11] B. Craps, D. Kutasov, and G. Rajesh, J. High Energy Phys. **06**, 053 (2002).

[12] M. Fabinger and J. McGreevy, hep-th/0206196.

[13] A. Lawrence, J. High Energy Phys. **11**, 019 (2002).

[14] G. T. Horowitz and J. Polchinski, Phys. Rev. D **66**, 103512 (2002).

[15] T. Banks, W. Fischler, S. H. Shenker, and L. Susskind, Phys. Rev. D **55**, 5112 (1997).

[16] J. M. Maldacena, Adv. Theor. Math. Phys. **2**, 231 (1998); Int. J. Theor. Phys. **38**, 1113 (1999).

[17] S. S. Gubser, I. R. Klebanov, and A. M. Polyakov, Phys. Lett. B **428**, 105 (1998).

[18] E. Witten, Adv. Theor. Math. Phys. **2**, 253 (1998).

[19] For a review of some recent developments see L. Rastelli, A. Sen, and B. Zwiebach, hep-th/0106010.

[20] E. Witten, Adv. Theor. Math. Phys. **2**, 505 (1998).

[21] V. Balasubramanian and S. F. Ross, Phys. Rev. D **61**, 044007 (2000).

[22] J. M. Maldacena, J. High Energy Phys. **04**, 021 (2003).

[23] V. E. Hubeny, hep-th/0208047.

[24] L. Susskind, L. Thorlacius, and J. Uglum, Phys. Rev. D **48**, 3743 (1993).

[25] W. Israel, Phys. Lett. **57A**, 107 (1976).

[26] G. T. Horowitz and D. Marolf, J. High Energy Phys. **07**, 014 (1998).

[27] V. Balasubramanian, P. Kraus, A. E. Lawrence, and S. P. Trivedi, Phys. Rev. D **59**, 104021 (1999).

[28] N. Goheer, M. Kleban, and L. Susskind, hep-th/0212209.

[29] J. M. Maldacena and A. Strominger, J. High Energy Phys. **12**, 005 (1998).

[30] M. Banados, C. Teitelboim, and J. Zanelli, Phys. Rev. Lett. **69**, 1849 (1992); M. Banados, M. Henneaux, C. Teitelboim, and J. Zanelli, Phys. Rev. D **48**, 1506 (1993).

[31] S. Hemming, E. Keski-Vakkuri, and P. Kraus, J. High Energy Phys. **10**, 006 (2002).

[32] M. Berkooz, B. Craps, D. Kutasov, and G. Rajesh, J. High Energy Phys. **03**, 031 (2003).

[33] G. T. Horowitz and D. L. Welch, Phys. Rev. Lett. **71**, 328 (1993); N. Kaloper, Phys. Rev. D **48**, 2598 (1993); A. Ali and A. Kumar, Mod. Phys. Lett. A **8**, 2045 (1993); M. Natsuume and Y. Satoh, Int. J. Mod. Phys. A **13**, 1229 (1998); Y. Satoh, Nucl. Phys. **B513**, 213 (1998); J. M. Maldacena and A. Strominger, J. High Energy Phys. **12**, 005 (1998); S. Hemming and E. Keski-Vakkuri, Nucl. Phys. **B626**, 363 (2002); J. Troost, J. High Energy Phys. **09**, 041 (2002); E. J. Martinec and W. McElgin, *ibid.* **04**, 029 (2002).

[34] E. Keski-Vakkuri, Phys. Rev. D **59**, 104001 (1999).

[35] L. Dyson, J. Lindesay, and L. Susskind, J. High Energy Phys. **08**, 045 (2002).

[36] A. Giveon, D. Kutasov, and N. Seiberg, Adv. Theor. Math. Phys. **2**, 733 (1998).

[37] J. M. Maldacena and H. Ooguri, J. Math. Phys. **42**, 2929 (2001); Phys. Rev. D **65**, 106006 (2002); J. M. Maldacena, H. Ooguri, and J. Son, J. Math. Phys. **42**, 2961 (2001); J. M. Maldacena and H. Ooguri, Phys. Rev. D **65**, 106006 (2002).

[38] J. Teschner, Nucl. Phys. **B546**, 390 (1999); **B571**, 555 (2000).

[39] A. J. Niemi and G. W. Semenoff, Ann. Phys. (N.Y.) **152**, 105 (1984).

[40] W. G. Unruh, Phys. Rev. D **14**, 870 (1976).

[41] C. P. Herzog and D. T. Son, J. High Energy Phys. **03**, 046 (2003).

[42] C. P. Burgess and C. A. Lutken, Phys. Lett. **153B**, 137 (1985).

[43] T. Inami and H. Ooguri, Prog. Theor. Phys. **73**, 1051 (1985).

[44] A. J. Tolley and N. Turok, Phys. Rev. D **66**, 106005 (2002).

[45] J. B. Hartle and S. W. Hawking, Phys. Rev. D **13**, 2188 (1976).